Current Trends in
Fashion Technology & Textile Engineering
ISSN: 2577-2929

Juniper Publishers
key to the Researchers

Short Communication
Volume 8 Issue 3- July 2023
DOI: 10.19080/CTFTTE.2023.08.555740

Curr Trends Fashion Technol Textile Eng

Discoloration of C.I. Reactive Red 120 Solutions by Electrochemical Treatment Using Anodic Electrodes of Al and Ti with and Pt without Surface Oxide Layer

Patermarakis G*

Department of Biomedical Engineering, University of West Attica, Greece

Submission: June 09, 2023; **Published:** July 13, 2023

***Corresponding author:** Patermarakis G, Department of Biomedical Engineering, School of Engineering, University of West Attica, Egaleo Park Campus, Greece, Email: gpaterm@uniwa.gr

Abstract

Solutions of azo-reactive dye red 120 were treated electrochemically using anodes in which oxide is formed, such as Al and Ti, and in which no oxide is formed, such as Pt in platinized Ti, Pt(Ti). Pb, Ti and Pt(Ti) correspondingly were used as cathodes in which the processes exert a marginal role. The systems Al – Pb and Ti – Ti showed significant efficiency in solution discoloration, ascribed mostly to active species formed in the anode. The discoloration of solution occurs in its bulk, rather than in electrode surfaces, and is accelerated by temperature rise. The Ti – Ti system is more effective regarding the rate of the process and the Al – Pb regarding the voltage and energy requirements, while the consumption of Al metal is much higher than that of Ti. Pt(Ti) – Pt(Ti) system is trivially effective. This different behavior is due to the different mechanism of oxygen-based active species release. In Al and Ti anodes where oxide grows, the release of electronic current and oxygen is an oxide lattice 3D process with a mechanism involving the formation of O-, O•, OH• and O3 dye-destructive species too. These are released in the interface, during the incessant renewal of a thin oxide layer interposed among the solution and metal and enter the attached layer and bulk solution. The oxygen evolution on Pt is a simpler 2D surface process, where all these species are not released or the release rates of all or some of them are much lower. Optimization of Al and Ti electrodes and other ones with oxides is expected to reveal highly effective methods for the destruction of azo-reactive dyes and final complete mineralization of related industrial effluents.

Keywords: C.I. Reactive Red 120 solutions; Electrochemical discoloration; Al–Ti–Pt anodes; Eco-friendly dyeing

Introduction

The discharge of industrial effluents containing textile-dye residuals, mainly into water-bodies recipients and secondly in soil ones, causes many serious environmental and health problems. These are generally toxic and carcinogenic. The contained dyes have a complex structure, mainly based on aromatic amines the partial degradation of which also generates various toxic by-products. The wastewater resulting from textile dyeing processes is very difficult to treat by the conventional activated sludge systems. Due to the non-biodegradable nature of the dyes, these in wastewater remain unaffected. Many different physicochemical methods were developed for the removal of dyes, e.g. coagulation/flocculation, adsorption on clay, perlite, activated carbon, carbon composites and biomaterials (algae, fungi, agricultural products and by-products, etc.) and other techniques such as reverse osmosis [1-3]. Recently a promising method was put forward [4] including the initial mixed physical and chemical adsorption on suitable adsorptive surfaces followed by coagulation/flocculation of dye and the subsequent recovery of separate dye and adsorptive material.

But, by the above methods [1-3] the contaminants, dyes and dye by-products, are transferred from one phase to another, or these are densified in the initial one, so the problem remains not completely solved [5-10]. The recovered dyes [4], if not reused, further require degradation and mineralization to simple molecules/ions H_2O, CO_2, N_2, NO_3^- etc., complicating the effluent processing practice. With the exception of reusable recovered dyes, in all other cases the destruction of dye and dye by-products and their mineralization within the effluents seems to be the best solution.

Suitable methods are the advanced oxidation processes (AOPs), that is the ozonation and other combined methods including ultra-violet (UV) radiation, H_2O_2 and O_3 (UV/H_2O_2, $UV/O_3/H_2O_2$). These can cause the destruction of chromophore groups in dye-molecule and discoloration of textile effluent. In the case of azo-reactive textile dyes the azo double bond –N=N– breaks initially, then intermediate colorless products are formed, e.g., nitrosamines. These products can be further degraded until their complete mineralization [11-14]. O_3 combined with radiofrequency alternating electric field (RFAEF), ultra-sound (US), UV and H_2O_2 (RFAEF/O_3, US/O_3, US/O_3/UV, US/O_3/H_2O_2) gave important synergetic results [1,15-17]. Pulsed power treatment techniques, that generate in situ strong oxidizing agents such as $OH^{\bullet}$, $H^{\bullet}$, $O^{\bullet}$, H_2O_2, O_2 and O_3, were successfully tested in azo-reactive dye effluents [18-21]. AOPs include electrochemical methods producing such active species. Mixed methods were also tried such as sono-electrocoagulation including sono-activation with electrochemical treatment, adsorption and coagulation/flocculation [22].

Despite a large amount of work done on the removal and destruction of dyes, a radical solution has not yet been achieved and the related research issue is still open. The detailed mechanisms of the destruction of chromophore groups and of the entire dye molecules up to mineralization become very complex when the specific chemical behaviors of separate rings, functional groups, atoms and substituents and the related elementary processes are considered. This complexity is enhanced considering the many different active species formed, e.g., during an electrochemical process.

A species involved in a dye destruction process may yield other intermediate species/radicals up to its final products. For example, considering O_3, $O_3 + H_2O \rightarrow HO_3^+ + OH^-$, $HO_3^+ + OH^- \rightarrow 2HO_2^{\bullet}$, $O_3 + HO_2^{\bullet} \rightarrow HO^{\bullet} + 2O_2$ [23], while it can partake in numerous other processes embracing many active species/radicals and also react directly with organic compounds [1]. The oxidative effect of the active species is not always clear. E.g., $OH^{\bullet}$ and $H^{\bullet}$ do not present only an oxidative behavior [24]. They can abstract H atoms from various organic compounds to form H_2 and H_2O molecules or can be added, e.g., to aromatic rings as a result of their electrophile character, where that of $H^{\bullet}$ is slight and of $OH^{\bullet}$ is more pronounced. Also, they can react with functional groups as a result of their redox properties. They react with inorganic compounds too. $H^{\bullet}$ behaves generally as a reducing agent, but there are exceptions where it behaves as an oxidizing agent, while the reaction $H^{\bullet} + OH^- \rightarrow e_{aq}^- + H_2O$, where e_{aq}^- is hydrated electron, may be looked upon as an acid-base process [24]. Other active species/radicals also show other complexities. A detailed description of the mechanisms and kinetics of all elementary and overall processes for dye discoloration/destruction is thus unfeasible.

A main reason for the necessity of discoloration is that the absorption of light hinders the bio-physicochemical processes that are vital for the eco-system in the recipient. Despite the difficulties in penetrating all those mechanisms, the discoloration that follows the break of –N=N– bond is easily studied. Moreover, the efficiency of further degradation of dye, to non-toxic and generally non-harmful fragments and to the complete oxidative degradation or mineralization, presumably follows that of discoloration, in view of which a first assessment of the employed methods can be made.

For an in-depth evaluation of an electrochemical method, the next issues are important: (i) The effect of the nature of electrode surfaces on dye discoloration/destruction, (ii) the space(s) where the discoloration occurs, (iii) the nature and amount of produced active species for each type of electrode and additive, and (iv) optimization of the entire process. Here, new electrochemical methods are employed using anodes Al, Ti and platinized titanium (Ti)Pt and cathodes Pb, Ti, and (Ti)Pt, enlightening as possible (i)–(iv), noting however that focus on the nature and precise amounts of active species for (iii) exceeds the scope of the study. The Al and Ti anodes, but not the Pt anode, always bear a well-developed oxide layer allowing the study of the presence of oxide on the effectiveness of dye discoloration.

Materials and Methods

Three of the most representative and commonly used azo-reactive dyes, most suitable for dyeing cotton and polyester/cotton blended fabric, are C.I. Reactive Yellow 84 (RY 84), C.I. Reactive Red 120 (RR 120) and C.I. Reactive Blue 98 (RB 198). These are anionic, highly soluble in water. The RR 120 (molar formula $C_{44}H_{24}Cl_2N_{14}O_{20}S_6Na_6$, molar mass 1469.98, and wavelength of maximum absorbance 535 nm) was chosen to avoid as explained before [4] long-lasting experiments and also for a better distinction of colors on the electrodes. Revealing any possible deposition of dye on the electrode surfaces is vital. Preliminary experiments showed that the red dye, if deposited, is more easily distinguished. The blue may resemble the oxide grown sometimes on Ti electrodes (see Results and Discussion, sections 2–4), thus it is not properly distinguished. Also, the yellow dye generally was not so efficiently discerned. Figure 1 shows the structural formula of RR 120 [25] and the color of dry dye deposited on a solid surface [4]. Some molecule size characteristics are: Representative dimension 2.48 nm, accessible area 14.84 nm^2, molecular area 8.83 nm^3 and solvent excluded volume 0.83 nm^3 [2]. A dissolved molecule of RR 120 gives an anion with charge -6 and six Na^+ ions.

An initial dye solution with concentration 50 mg dm^{-3} (or 3.4014×10^{-5} mol dm^{-3}) and pH = 6.75 was used. The charge density of dye anion is thus 19.691 C dm^{-3}. To clarify the effect of the electrodes used on the discoloration of dye solution, ideally no other compound should be added. But the experiments without additives needed high voltage (ΔV) and high energy consumption due to the low conductivity of dye solution. Additives rising it, but ***not affecting as possible*** the mechanisms of the processes on the electrodes, should be used. For this purpose, an amount of the chosen solid additive was added in the dye solution, so the noted

How to cite this article: Patermarakis G. Discoloration of C.I. Reactive Red 120 Solutions by Electrochemical Treatment Using Anodic Electrodes of Al and Ti with and Pt without Surface Oxide Layer. Curr Trends Fashion Technol Textile Eng. 2023; 8(3): 555740. DOI: 10.19080/CTFTTE.2023.08.555740

here concentration is close to the real one, or certain volumes of dye and additive solutions of known concentrations were mixed and the noted concentration is the exact. Experiments were designed to clarify, as much as possible, the earlier noted issues (i)–(iv).

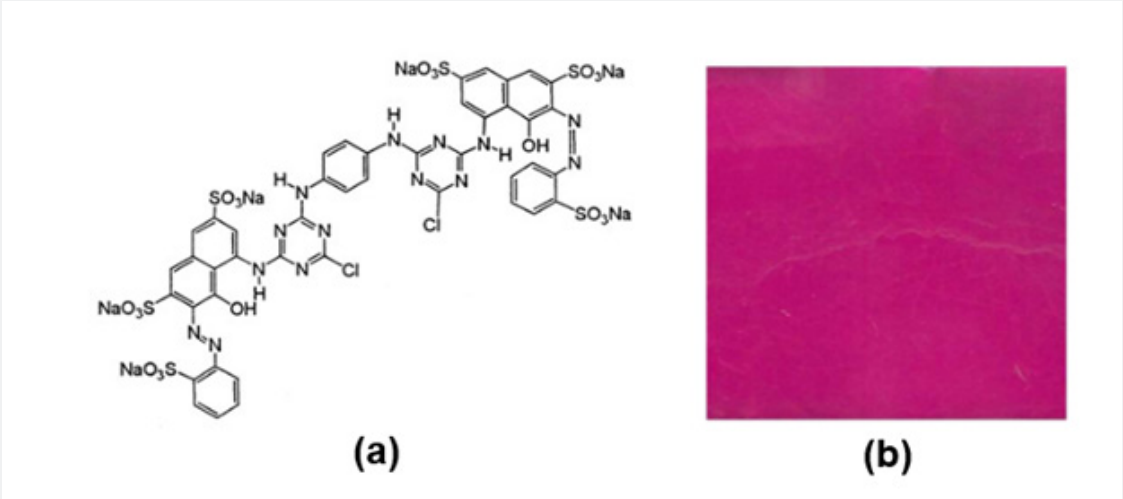

Figure 1: (a) Structure of C.I. Reactive Red 120 (RR 120) dye [25]. (b) The physical color of a multimolecular solid layer of dye taken up from its solution by the surface of porous anodic alumina film after drying the entire system [4].

The electrodes used were sheets of Al (purity ≥ 99.9518%, Merck pro-analysis), Pb (purity ≥ 99.968%, Merck pro-analysis) and Ti (purity 99%, Alfa Aesar), all of thickness 0.5 mm, and platinized Ti, Pt(Ti), with Pt thickness 2 μm on Ti 0.5 mm thick. The conductive surface was 5×5 cm^2. Each electrode had a stem 5×1 cm^2, originating from the center of a side. It was insulated except of its bare upper edge with length 1 cm for the electrical connection, Figure 2. The conductive geometric surface area of Al, Pb, Ti and Ti(Pt) electrodes was S_g = 50.95 cm^2. Current (I) = 0.5 A, or current density (j) = 9.91 mA cm^{-2}, was applied. The distance among anode and cathode, mounted vertically, was 5 cm.

A homemade power supplier was used working galvanostatically or potentiostatically with upper limits of power output ≈ 50 W, current (I) = 2 A and $\Delta V \approx$ 35 V (PS_1). For higher ΔVs, another power supplier was used where I and ΔV are manually regulated (PS_2). The anodic potential (> 0) and cathodic one (< 0) were measured by Hg/Hg_2SO_4 reference electrode with P_{ref}(vs. SHE) = 0.615 V at 25 °C [26]. Then P_{an}(vs. SHE) and P_{ca}(vs. SHE), or P_{an} and P_{ca}, can be found.

f2

The solution, Figure 2, was thermostated by setting the temperature of circulating heating/cooling fluid (T_f) at 25 °C, except otherwise noted. At low ΔVs and high volumes of solution, the temperature (T) of solution and electrodes was ≈ 25 °C. At high ΔVs and low volumes of solution, T could rise during electrolysis, allowing however important observations. The solution was magnetically stirred at a low nominal rate 2 (max 10) to avoid violent mixing of solution and air, which could uncontrollably affect the dye-destructive species and processes. A UV/VIS Hitachi U-1100 spectrophotometer and reference plot, absorbance vs. concentration, were used to follow the discoloration of solution.

The conductivity of dye solution (κ_d) at concentration (c_d) = 50 mg dm^{-3} and T = 25 °C was found 5.952×10^{-3} ohm^{-1} m^{-1}, not much higher than that of used deionized water 4.27×10^{-4} ohm^{-1} m^{-1}. For comparison, that of pure water is 6.414×10^{-6} ohm^{-1} m^{-1} [26]. The unknown mobility of bulky dye anions must be negligible compared with that of Na^+ and the κ_d is thus mostly due to the mobility of Na^+. For such low c_ds, the Bjerrum activity coefficient should tend to 1 [27]. The concentration of Na^+ is $6c_d$. Ignoring the mobility of dye anions and assuming this coefficient 1, then at c_d = 50 mg dm^{-3} and T = 25 °C, $\kappa_d \approx 1.029\times10^{-2}$ ohm^{-1} m^{-1} that is expected to be only slightly lower than the real κ_d. The measured conductivity is 57.9% of 1.029×10^{-2} ohm^{-1} m^{-1}. So, this coefficient is < 0.58, indicating strong Debye-Hückel interactions and/or that some secondary equilibrium process(es) embracing ionic species is (are) set up. For other c_ds in a narrow range around 50 mg dm^{-3}, the κ_d was found considering reasonably that it is proportional to c_d, Table 1.

As explained below, the appropriate additive is Na_2SO_4. The conductivities of its solutions (κ_s), Table 1, were found from literature data of κ_ss at certain concentrations (c_s) and 18 °C and temperature coefficients [26] by interpolation. At the used c_ss, κ_ds << κ_ss. Thus, when Na_2SO_4 additive is present, calculations are made using κ_s.

How to cite this article: Patermarakis G. Discoloration of C.I. Reactive Red 120 Solutions by Electrochemical Treatment Using Anodic Electrodes of Al and Ti with and Pt without Surface Oxide Layer. Curr Trends Fashion Technol Textile Eng. 2023; 8(3): 555740. DOI: 10.19080/CTFTTE.2023.08.555740

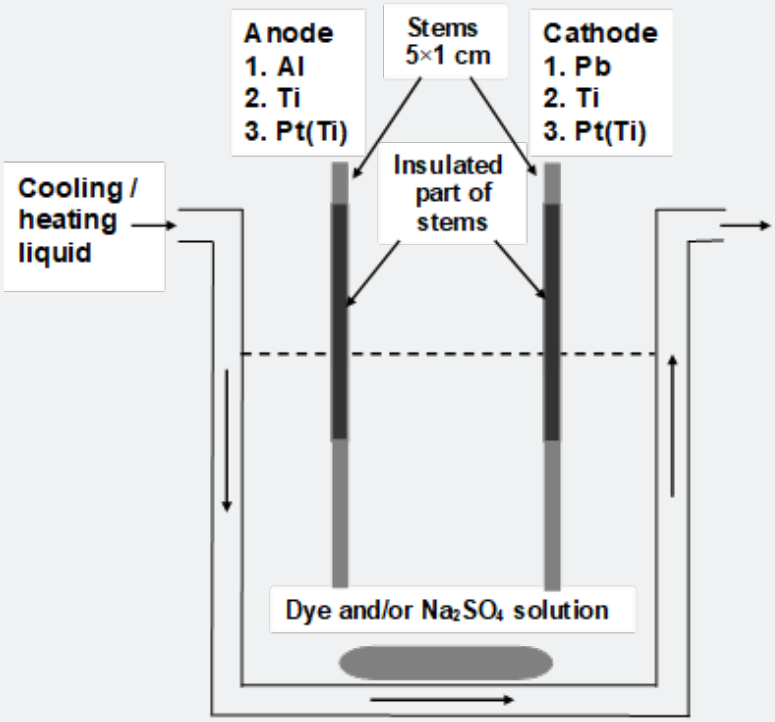

Figure 2: Electrolytic cell setup for the electrolysis of dye-containing solutions with the use of three different pairs of anodic and cathodic electrodes.

Table 1: Conductivities of separate dye solutions, κ_d, and Na_2SO_4 solutions, κ_s, at various concentrations of dye RR 120, c_d, and Na_2SO_4, c_s.

Compound	c_d/mg dm^{-3}	c_d/mol dm^{-3}	T/°C	κ_d/ohm^{-1}m^{-1}
RR 120	47.5	3.231×10^{-5}	25	5.654×10^{-3}
RR 120	48.077	3.271×10^{-5}	25	5.723×10^{-3}
RR 120	50	3.401×10^{-5}	25	5.952×10^{-3}
Compound	c_s/g dm-3	c_s/mol dm^{-3}	T/°C	κ_s/ohm^{-1}m^{-1}
Na_2SO_4	5.391	0.0385	25	0.603
Na_2SO_4	7.001	0.05	25	0.762
Na_2SO_4	7.001	0.05	57	1.256
Na_2SO_4	14.002	0.1	25	1.439
Na_2SO_4	23.341	0.1667	25	2.308
Na_2SO_4	140.02	1	25	10.006
Na_2SO_4	140.02	1	62	18.020

Results and Discussion

Al anode – Pb cathode

Electrochemistry of oxide growth on the Al anode: Al is covered by a rapidly formed native passive oxide film with limiting thickness 2-3 nm [28]. When Al is anodized in pore forming electrolytes, e.g. oxalic, sulfuric, phosphoric, tartaric, etc. acid, initially it thickens and finally porous anodic alumina films (PAAFs) grow [29]. Their growth occurs in three sequential stages, the first and second short transient stages and the third steady-state stage that is desirably short or long where the structure of PAAFs become close-packed array of about hexagonal columnar cells [30-33]. Each cell contains an elongated pore vertical to the Al surface, extending from the top surface to near the Al|oxide

How to cite this article: Patermarakis G. Discoloration of C.I. Reactive Red 120 Solutions by Electrochemical Treatment Using Anodic Electrodes of Al and Ti with and Pt without Surface Oxide Layer. Curr Trends Fashion Technol Textile Eng. 2023; 8(3): 555740. DOI: 10.19080/CTFTTE.2023.08.555740

interface, while a thin spherical sector shell-shaped barrier-type layer with thickness ≈ 1 nm per V of Δ*V* exists among the interface and pore bottom [30-33]. Al anodizing in H_2SO_4 needs lower Δ*V* and produces PAAFs with surface density of pores of the order 10^{10} cm^{-2} and pore base diameter of the order of up to about 10 nm [33]. Figure 3 shows some structural details of PAAF formed in H_2SO_4 [34].

To study the discoloration of dye solution, Al could be anodized in a similar acidic solution, e.g. 0.51 M [34], containing dye. But, its low pH ≈ 0.3 [26] could affect the structure of dye anion and the mechanism of solution discoloration. Also, concerning the industrial effluents, after discoloration their neutralization and additional treatment to remove the sulphates present at significant concentration are needed before their disposal. Thus, Al anodizing in dye solution at pH close to 7 was chosen. Oxide growth is also possible in an electrolyte at pH ≈ 7 when its anion does not decompose under the action of the electric field in the anode|electrolyte interface. Initially non-porous anodic alumina film is formed. If the oxide is not dissolved or Al^{3+} ions cannot at all be solvated, the thickness of non-porous oxide increases about linearly with Δ*V*, when the current is left to decline to near zero, up to ≈ 1.4 nm V^{-1} [31,32].

If constant *I* is applied, the required Δ*V* increases with time up to hundreds V. Such type of Al anodization is unsuitable here. If the solution dissolves slightly the oxide or, equivalently, Al^{3+} ions are ejected in the solution by the field and/or by oxide dissolution and solvated, the initial non-porous oxide can be then transformed to porous. Such electrolyte is Na_2SO_4.

For *I* or Δ*V* above some limits that depend on *T*, type and concentration of electrolyte, etc., the uniform normal PAAF growth turns locally to abnormal and burning emerges [35]. It is a much faster local film growth associated with higher local *j* and real *T* around the barrier layer and altered structural parameters, e.g. thinner barrier layer that is related to altered surface pore density, pore diameter and pore wall thickness around the pore bases. The presence of Na_2SO_4 is expected to eliminate this abnormal growth or to suppress it to some extent if it occurs, mostly at high c_ss.

The current in the growing non-porous film or in the barrier layer of growing PAAF (I_a) is $I_a = I = I_{a,a} + I_{a,c} + I_{a,e}$, Figure 4. $I_{a,a}$ is the anionic current through it due to O^{2-} anions that migrate to the Al side to form oxide, mainly in the metal|oxide interface and maybe partly within the oxide and in the oxide|electrolyte interface, at faradaic rate as regards $I_{a,a}$. O^{2-} ions are formed in the latter interface by the dissociative adsorption of H_2O and ejection of H^+ to the anolyte [35]. $I_{a,c}$ is the cationic current due to migration and ejection of Al^{3+} ions. It exists only if Al^{3+} ions can be solvated, otherwise $I_{a,c} = 0$. In the outer oxide sublayer minor amounts of $Al_2(SO_4)_3$ and/or AlOOH and/or $Al(OH)_3$ can be formed by migrating Al^{3+} and the contaminant electrolyte anions, OH^- and H^+ that are embodied in it. $I_{a,e}$ is the electronic current through the oxide related to the formation inside it and in the oxide|electrolyte interface by a specific mechanism [36] of species O^-, $O^\bullet$ and O_2 containing a small fraction of O_3. It includes certain processes that follow the polarization and destabilization, under the action of high field, of the large O^{2-} ions with radius 0.14 nm [37] instead of the small Al^{3+} ions with radius 0.053 nm [37] placed in spaces between O^{2-}. In the above sublayer and interface, $O^- + H^+ \rightarrow OH^\bullet$, can also occur. The rates of O^-, $O^\bullet$, $OH^\bullet$ and O_3 release must follow that of O_2.

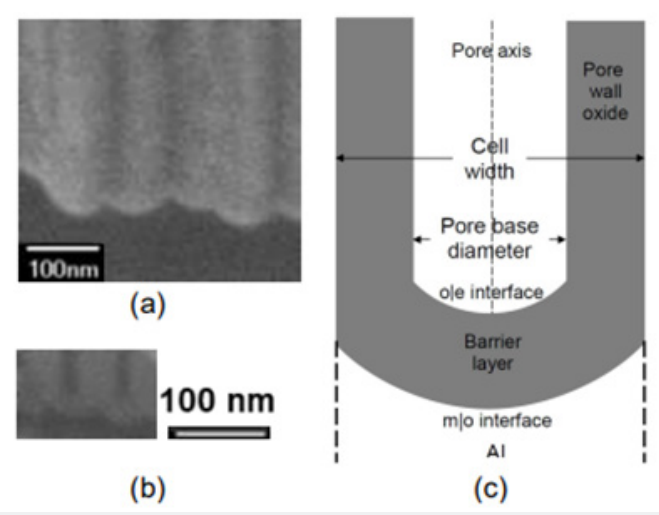

Figure 3: (a, b) Field emission scanning electron microscopy (FESEM) micrographs of the cross-sectional fractures of PAAFs formed in 0.51 M H2SO4 electrolyte at anodic potential (vs. SHE) 23.615 V, temperature 298 K and electrolysis times 2430 s (a) and 2280 s (b) where the current density is 212.9 mA cm-2 and 43.3 mA cm-2, respectively, [34]. (a) External geometry of the columnar cells detached via intercellular boundaries and of the corresponding barrier layer units in a region near Al substrate. (b) Cross section of spherical-sector shell-shaped barrier layer units. (c) Schematic cross section of a cell/pore unit of PAAF around the pore base region where the pore, its axis, pore wall, barrier layer, cell width and pore base diameter are shown.

How to cite this article: Patermarakis G. Discoloration of C.I. Reactive Red 120 Solutions by Electrochemical Treatment Using Anodic Electrodes of Al and Ti with and Pt without Surface Oxide Layer. Curr Trends Fashion Technol Textile Eng. 2023; 8(3): 555740. DOI: 10.19080/CTFTTE.2023.08.555740

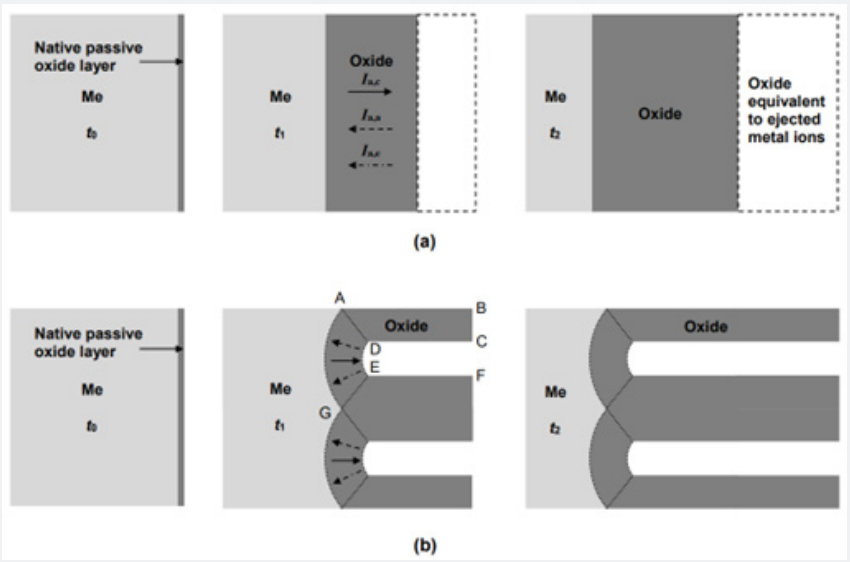

Figure 4: Schematic of anodic oxide growth on Al or Ti metal (Me) when (a) non-porous and (b) cellular columnar porous oxide is formed, in suitable electrolyte and conditions for each metal, at times t0, t1 and t2 (t0 = 0 < t1 < t2), where t1 and t2 for the porous layer are small but within the quasi-steady state stage. For the non-porous oxide, a layer equivalent to the ejected metal cations, mainly electrochemically and secondarily chemically, is shown. For the porous oxide its volume about equals that of pores, CDEF. The Ia,e is related to the formation of O-, O•, OH•, O3 and O2 species within the non-porous oxide and the barrier layer of porous oxide, ADEH, and in the oxide|electrolyte interface, DE. Those formed in the interface are released directly in the solution and those in the non-porous oxide or in the barrier layer of porous oxide are subsequently released, as they are renewed continuously [36]. Those enclosed in the pore walls are released as they are chemically dissolved slowly during the oxide growth and the pores open up outwards that is detected mainly at high t's and thus not shown here.

During PAAF growth these species formed in the oxide|electrolyte interface are released directly in the pore filling solution. Those existing in the barrier layer and pore walls are released during the continuous renewal of the barrier layer and the chemical dissolution of pore walls [36]. Then, these are transferred to the attached layer and bulk solution. Depending on the anodizing conditions, the release rate of O_2 (containing O_3) varies from low, hardly detected as here, to high equivalent to a significant portion of I [36]. The O^-, $O^\bullet$ and $OH^\bullet$ are short-lived, thus short-range acting, but the dissolved O_3 is relatively long-lived and long-range acting, partaking in various processes.

Since the solution becomes alkaline during the electrolysis and Al is attacked by alkaline solutions, the Al cathode could give products additional to those obtained from the Al anode. This would cause confusion as to the origin of dye solution discoloration. So, Pb was used as cathode which is slowly attacked only in hot acidic sulphate solutions [38]. In Pb cathode H_2 is released. Short-lived and short-range acting $H^\bullet$ radicals can be formed, located mainly in the surface and attached layer and much less in the catholyte. The $H^\bullet$, acting in various ways [24], could destroy or not the chromophore groups of dye anions and cause fragmentation with either conservation or not of that groups. But most probably $2H^\bullet \rightarrow H_2$ almost solely occurs. Also, the approach of dye anions to the (-) charged cathode is hindered, thus any effect of $H^\bullet$ to dye solution discoloration, if existing, must be trivial. The rate of H_2 release is thus closely faradaic. Some secondary processes may occur in the vicinity of cathode starting from the dissolved O_2 [23], $O_2 + H_2O + 2e^- \rightarrow HO_2^- + OH^-$, $HO_2^- \rightarrow OH^- + O^\bullet$, $HO_2^- + H_2O + 2e^- \rightarrow 3OH^-$, giving active species for dye destruction.

At the employed j, $I_{a,e}$ in the Al anode is very small and the release of oxygen occurs at a very low rate [36], thus it is a minor process. $Al_2(SO_4)_3$, AlOOH and $Al(OH)_3$ possibly formed in minor amounts in the oxide space just next the oxide|electrolyte interface are ignored. Then, the Al oxidation is nearly faradaic according to the process [35].

$$Al + tn_{an}(3/2)H_2O \rightarrow tn_{an}(1/2)Al_2O_3 + tn_{an}3H^+_{aq,h} + tn_{ca}Al^{3+}_{aq,h} + (tn_{an} + tn_{ca})3e^-, \quad (1)$$

where tn_{an} and tn_{ca} ($tn_{an} + tn_{ca} = 1$) are the transport numbers of O^{2-} and Al^{3+} in the non-porous film or in the barrier layer of PAAF and $Al^{3+}_{aq,h}$ is hydrated and solvated Al^{3+}. In the Pb cathode and acidic solution H_2 is released by the reaction

$$2H^+_{aq,h} + 2e^- \rightarrow H_2, \quad (2)$$

in alkaline it is released by $2H_2O \rightarrow H_2 + OH^-_{aq,h}$ [27] and in neutral reasonably by both. In view of reaction,

How to cite this article: Patermarakis G. Discoloration of C.I. Reactive Red 120 Solutions by Electrochemical Treatment Using Anodic Electrodes of Al and Ti with and Pt without Surface Oxide Layer. Curr Trends Fashion Technol Textile Eng. 2023; 8(3): 555740. DOI: 10.19080/CTFTTE.2023.08.555740

$$H_2O \rightleftharpoons H^+_{aq,h} + OH^-_{aq,h}, \quad (3)$$

always taking place, (2) can be considered to occur equivalently in each type of solution and the consumption of $H^+_{aq,h}$ in cathode is faradaic. From the consumed $H^+_{aq,h}$ ions per mol of reacting Al, the part $3tn_{an}$ comes from the reaction (1) and the part $3tn_{ca}$ comes from the additional H_2O decomposition. The overall process in both anode and cathode is then

$$Al + tn_{an}(3/2)H_2O + 3tn_{ca}H^+_{aq,h} \rightarrow tn_{an}(1/2)Al_2O_3 + tn_{ca}Al^{3+}_{aq,h} + (3/2)H_2. \quad (4)$$

In not highly alkaline solution, the anodic behavior of Al resembles that in not highly acidic and in neutral solution, although the processes that follow may differ. At given I and T, the potential drop in the non-porous film or in the barrier layer of PAAF, or P_{an}, is about proportional to its thickness by ≈ 1 V nm^{-1} [30-33]. 200 ml of solution with c_d = 47.5 mg dm^{-3} and c_s = 0.05 mol dm^{-3} (0.7% w/v) was used. Na_2SO_4 changes the pH in pure H_2O by ΔpH = 0.5pK_a + 0.5logc_s ≈ 0.31, where K_a = 1.2×10^{-2} is the second dissociation constant of H_2SO_4 (the first is complete) [26]. In the dye solution with pH 6.75, its change must also be ≈ 0.31. Really, 6.75 + 0.31 = 7.06 ≈ 7.03 measured. The Na^+ ions in this solution are not deposited, sulfate anions do not decay and Al^{3+} ions are solvated, so PAAF can also be formed. These anions are also relative to sulfonic groups in dye anions. Na_2SO_4 is thus almost indifferent to discoloration processes.

Discoloration of dye solution during electrolysis

The dye solution was electrochemically treated at I = 0.5 A using PS_1 and up to t = 2 hours at which complete discoloration was achieved. T increased from 25 to ≈ 57 °C until about 1 hour and then remained almost stable. Due to the small volume of solution and surface of heat exchange and the low stirring rate, the rate of heat release in the solution exceeds that of heat abduction at low Ts. A balance is reached at T ≈ 57 °C. ΔV varied from ≈ 34.0 V at the start of electrolysis to ≈ 24.3 V at t = 1–2 hours. ΔV is shared to P_{an} > 0, potential drop in the bath solution (ΔV_{bs} > 0) and -P_{ca} > 0. From P_{ca} vs. j data for H_2 evolution on Pb cathode [34], P_{ca} ≈ -1.15 V at 25 °C.

From κ_s, Table 1, the dimensions and distance of electrodes, ΔV_{bs} can be estimated. At 25 °C, ΔV_{bs} ≈ 6.56 V. $P_{an} = \Delta V - \Delta V_{bs} + P_{ca}$ ≈ 26.29 V, thus the non-porous film or the barrier-layer in PAAF has a thickness ≈ 26 nm. After electrolysis pH = 10.97 (25 °C). During it, the composition of solution changes, pH and T rise and ΔV falls, so P_{an}, ΔV_{bs} and P_{ca} change too. Mainly due to T and secondarily to pH rise, κ_s at 57 °C is higher. From κ_s at this T, ΔV_{bs} is estimated ≈ 3.98 V, while 0 > P_{ca} > -1.15 V [34]. So, 20.31 V > P_{an} > 19.17 V and the predicted thickness of non-porous film or of barrier layer in porous film is roughly ≈ 20 nm. By a non-destructive method [39] a mean film thickness of several μm was found. Thus, the entire film resembles PAAF, Figure 3. Due to T rise, tn_{an} and tn_{ca} in barrier layer change [40] and the structural and kinetic parameters change with T and t [34], but their study exceeds the scope of this work.

After electrolysis, a white to grayish-white precipitate was observed. Due to the contained sulphate ions and pH > 7, it must be a mixture of white $Al(OH)_3$ [41] and grayish-white $Al_2SO_4(OH)_4 \cdot 7H_2O$ (aluminite), where aluminite seems to predominate. Aluminite could cage a dye amount, which is excluded since it did not take any blushing hue.

The H^+ ions are provided by the reaction (3) and consumed by (4), while a surplus of $OH^-_{aq,h}$ appears. The solvated Al^{3+} ions form various complex cations [41,42] and/or $Al(OH)_3$ [41] and aluminite, all of which include OH^-. The $H^+_{aq,h}$ and $OH^-_{aq,h}$ concentrations are regulated by the reactions (3) and (4), the ionic product of H_2O, k_w = 1.27×10^{-14}–10.5×10^{-14} at 25–57 °C [26] and by the above processes consuming OH^-. So, an exceeding rise of pH is prevented.

The initial charge (Q) of dye anions 3.74 C is negligible compared to the passed Q = 3600 C. This indicates that the discoloration does not occur on the Al anode surface, but mostly in the bulk solution. The O^-, $O^\bullet$, $OH^\bullet$, O_2 and O_3 released in the solution and some their by-products destroy the chromophore groups [18-21]. While O^-, $O^\bullet$ and $OH^\bullet$ are short-lived and short-range acting, like $H^\bullet$, O_3 is long-lived, long-range acting and thus more effective. As a whole the destructive species formed in the anode must be much more active than $H^\bullet$ in the cathode. Other color observations:

Al anode: It became red-violet (magenta) in certain linear upwards very small and rare regions with negligible area. Locally, advanced burning emerged tending to electropolishing, eventually a thin almost planar film [36] with thickness roughly around 20 nm remained, the local js exceeded the mean 9.91 mA cm^{-2} and the release of oxygen and related species was reinforced. Thin anodic films often show interference colors [43] among which is magenta. It does not originate from the dye that is adsorbed very slowly on PAAF [4] or from electro-adsorbed anions as their large size and stereoscopic arrangement of absorbable atoms, substituents and functional groups do not favor stable electro-adsorption.

The attached layer is enriched with dye-destructive species. When dye anions approach it, the chromophore groups are destroyed. Thus, the discoloration of dye solution practically occurs in the liquid phase. If dye anion fragments are formed, due to its high charge, these are also expected to be anionic or at most neutral. When colored fragments approach this layer, they are destroyed too. Access of bulky anions to the anode and their adsorption is hindered and prevented, more so in burning/electropolishing positions where active species are released faster [36].

Pb cathode: During electrolysis its color remained unchanged indicating that the dye is not adsorbed on its surface.

How to cite this article: Patermarakis G. Discoloration of C.I. Reactive Red 120 Solutions by Electrochemical Treatment Using Anodic Electrodes of Al and Ti with and Pt without Surface Oxide Layer. Curr Trends Fashion Technol Textile Eng. 2023; 8(3): 555740. DOI: 10.19080/CTFTTE.2023.08.555740

Ti anode – Ti cathode. Electrochemistry of oxide growth in the Ti anode and discoloration of dye solution

Electrolysis of water with Ti electrodes gives it highly disinfecting properties [23,44], attributed to certain lethal for the bacteria processes in the Ti electrodes and water bulk and to processes producing oxidizing/lethal species in the anode including O_3 and its by-products [23] that exert a key effect. So, Ti electrodes were used also here. The Ti surface bears a native TiO_2 passive layer 1.5–10 nm [45,46] reaching at prolonged exposure 25 nm [47] or more that is taken here the initial mean TiO_2 thickness. The anodic behavior of Ti and Al somewhat resembles at suitable conditions [31], Figure 4.

The oxidation of n_1 mol Ti in the anode is described as

$$n_1(\mathrm{Ti} + tn_{an}2H_2O \rightarrow tn_{an}TiO_2 + tn_{an}4H^+_{aq,h} + tn_{ca}Ti^{4+}_{aq,h} + 4e^-) \quad (5)$$

where $Ti^{4+}_{aq,h}$ is hydrated Ti^{4+}. The $n_1 4tn_{an}H^+$ mol are discharged in the cathode. The rest H^+ ions that are discharged come from the oxidation of n_2 mols of H_2O in the anode

$$n_2H_2O \rightarrow (1/2)n_2O_2 + 2n_2H^+_{aq,h} + 2n_2e^- \quad (6)$$

The combination of (5) and (6) processes gives

$$n_1\mathrm{Ti} + n_1tn_{an}2H_2O + n_2H_2O \rightarrow n_1tn_{an}TiO_2 + n_1tn_{ca}Ti^{4+}_{aq,h} + n_2(1/2)O_2 + (n_1tn_{an}4 + n_2 2)H^+_{aq,h} + (4n_1 + 2n_2)e^- \quad (7)$$

Considering a faradaic discharge of H^+ in the cathode, then

$$(4n_1 + 2n_2)H^+_{aq,h} + (4n_1 + 2n_2)e^- \rightarrow (2n_1 + n_2)H_2 \quad (8)$$

Ignoring other secondary processes in the anode and cathode, the combination of (7) and (8) gives the overall process

$$n_1\mathrm{Ti} + (2n_1tn_{an} + n_2)H_2O + 4n_1tn_{ca}H^+_{aq,h} \rightarrow n_1tn_{an}TiO_2 + n_1tn_{ca}Ti^{4+}_{aq,h} + n_2(1/2)O_2 + (2n_1 + n_2)H_2. \quad (9)$$

The $2n_1 + n_2$ is related to Q by $(4n_1 + 2n_2)F = Q = Q_{Ti} + Q_w$, where F is Faraday's constant and $Q_{Ti} = 4n_1F$ and $Q_w = 2n_2F$ are the charges consumed by Ti and H_2O oxidation, reactions (5) and (6). Reaction 9 is rewritten as

$$\mathrm{Ti} + (2tn_{an} + n_2/n_1)H_2O + 4tn_{ca}H^+_{aq,h} \rightarrow tn_{an}TiO_2 + tn_{ca}Ti^{4+}_{aq,h} + (n_2/n_1)(1/2)O_2 + (2 + n_2/n_1)H_2, \quad (10)$$

Since the main process here is the decomposition of H_2O (see below) then $n_2/n_1 >> 1$.

In the TiO_2 of anode, Ti^{4+} ions with radius 0.06 nm [37] are small compared to O^{2-}, Ti^{4+} ions are ejected in the solution and the oxide layer is incessantly renewed. So, oxygen evolution will occur by a mechanism similar to that for Al anode [36]. O^-, $O^\bullet$, $OH^\bullet$, O_3 and O_2 enter the attached layer and solution and the rates of O^-, $O^\bullet$, $OH^\bullet$ and O_3 release follow that of O_2. The composition of O^-, $O^\bullet$, $OH^\bullet$, O_3 and O_2 system and the released amounts must differ from those for Al where $I_{a,e}$ is much lower. In the Ti cathode, besides H_2 release, $H^\bullet$ formation [24] and processes involving $H^\bullet$ and dissolved O_2 (section 1.1), other secondary ones can also occur. These are the reduction of TiO_2 to Ti, $Ti^{4+} + 4e^- \rightarrow Ti$ and $4H^+_{aq,h} + 2O^{2-} \rightarrow 2H_2O$ decreasing the thickness of TiO_2, and/or to other oxide(s) such as Ti_6O, Ti_5O, Ti_3O, Ti_2O, TiO, Ti_2O_3, Ti_3O_4 and Ti_3O_5 [48] with oxidation number of Ti < 4, $TiO_2 + ne^- + nH^+_{aq,h} \rightarrow Ti^{4-n}O_{(4-n)/2} + (n/2)H_2O$.

The overpotential of H_2 release in the Ti cathode obeys Tafel equation $-P_{ca} = a + b\log j$ (j/A cm^{-2}), where at 20 °C a = 0.82 and b = 0.14 in acidic and a = 0.83 and b = 0.14 in alkaline solutions [27]. Thus, it is almost unaffected by pH, in neutral solution $-P_{ca}$ = 0.825 + 0.14log$j$, and at j = 9.91 mA cm^{-2} $-P_{ca}$ = 0.544 V. It is assumed that this is the value of $-P_{ca}$ when the thickness of the oxide layer on Ti tends to zero. As in Pb [34] and other metal [27] cathodes, $-P_{ca}$ must fall very slightly with T. Thus, its value at 20 °C is also adopted for 25 °C, without damaging the analysis. P_{an} includes the potential drop across the oxide layer in the anode and the oxygen evolution potential, and $-P_{ca}$ includes the potential drop across this layer possibly existing in the cathode and the hydrogen evolution potential. At given j and T, P_{an} and $-P_{ca}$ obviously increase with the thickness of oxide layer on the electrodes.

200 ml of dye solution with c_d = 50 mg dm^{-3} was electrochemically treated at I = 0.5 A using PS_2 for t = 30 min. Initially ΔV was ≈ 150 V, then it increased in the range ≈ 150–170 V by a fluctuating mode. T increased from 25 to ≈ 62 °C until t = 30 min. From κ_d at 25 °C ΔV_{bs} is estimated >> 150 V. But, at the start $\Delta V \approx 150$ V > ΔV_{bs}. At high voltages and pH ≈ 7, the mechanism of electrical conduction may become more complicated than simple migrations of Na^+, dye anions, H^+ and OH^-, but its elucidation is outside the scope of this study. At given T, the thickness of pre-existing oxide in the Ti anode (cathode) must increase (decrease) by the oxidation (reduction) processes on them, thus it depends on t and T. ΔV changes as a result of conductivity rise and ΔV_b fall with increasing T, change of P_{an} and $-P_{ca}$ with t and T, and growth of pitting corrosion in the anode (section 4) that seems related to the increase of ΔV by a fluctuating mode.

To reduce ΔV, at t = 30 min an amount of Na_2SO_4 to $c_s \approx 1$ M was added. It was rapidly dissolved and ΔV fell to 5–6 V. Then T was kept at ≈ 62 °C by adjusting T_r. At t = 30 min the discoloration was ≈ 35% and at t = 60 min complete. The concentrations of dye-destructive species must rise with t, maybe up to some limits depending on T. Increasing their concentrations and T hasten the discoloration, also indicating mainly chemical processes. The release of oxygen and hydrogen was intensive at all ts. So, the decomposition of H_2O is the main process. When oxide exists in anode and cathode the current through it is mainly electronic, and not ionic which needs higher field for given current.

For not appreciable change of pH (as, e.g., in section 4) and of solution composition up to t = 60 min, from κ_s, Table 1, ΔV_{bs} is

How to cite this article: Patermarakis G. Discoloration of C.I. Reactive Red 120 Solutions by Electrochemical Treatment Using Anodic Electrodes of Al and Ti with and Pt without Surface Oxide Layer. Curr Trends Fashion Technol Textile Eng. 2023; 8(3): 555740. DOI: 10.19080/CTFTTE.2023.08.555740

estimated ≈ 0.5 and ≈ 0.277 V at 25 and 62 °C. Assuming that at T = 62 °C the oxide thickness in the cathode tends to zero, then 0 < $-P_{ca}$ < 0.544 V [27] and 4.179–4.723 V < P_{an} < 5.179–5.723 V. P_{an} includes the potential drop across the TiO_2 film and potential of oxygen release that exceeds the equilibrium one 0.7639 V at this T and pH = 7 [49]. Adopting a field strength across it roughly ≈ 1 V nm^{-1} (as for Al anodic oxide), then its final thickness is ≈ 4.5–5.5 nm which is too small for Ti anode compared with that of initial passive layer. As the current through it is mostly electronic, this field must be somewhat < 1 V nm^{-1}, depend on T and be different in the anode and cathode. Thus, $-P_{ca}$ can be higher and P_{an} lower than the above, with thicknesses of oxide in anode and cathode >> 4.5–5.5 nm and >> 0. Even in the anode it is negligible compared to the faradaic 17.34 μm found for TiO_2 (rutile) density 4.26 g cm^{-3} [38].

Due to the increase of ΔV and decrease of ΔV_{bs} and $-P_{ca}$ as T rose, P_{an} and the mean oxide thickness must have increased enough up to 30 min. But after the addition of Na_2SO_4 its thickness decreased. Ti is attacked only by acids [38], but this does not exclude the solvation of Ti^{4+} ions in neutral solution. The thinning of oxide in the anode after adding Na_2SO_4 verifies the solvation of Ti^{4+}. $Ti(SO_4)_2$ is an existing compound [42,50] and the sulphate ions at high concentration promote the solvation of Ti^{4+} mainly at high Ts despite that the main process is still the release of oxygen.

Despite the very much higher ΔV for Ti up to 30 min than for Al up to t = 60 min (section 1.2), the T peaks at these ts differ by only 62 - 57 = 5 °C. Thermochemical analysis showed that the reaction (4) is moderately exothermic and (10) is highly endothermic, but the corresponding rates of heat release and absorption are low. For, e.g., tn_{an} = 0.5–0.7 it is only 3.64–4.51% (Al) and 0.72–0.73% (Ti) of IΔV [51]. This must occur also for all other possible reactions that follow (4) and (10). T depends mainly on IΔV and the rate of heat abduction. The release of gas in the Ti anode at higher enough rate causes extra stirring beyond the light one applied, favoring more heat removal for this system. All these factors result in a difference of T peaks limited to 5 °C. Additional color observations:

Anodic Ti electrode: The whole area of the side in front of cathode (internal side) became blue. The other side was partially colored blue. Bluer color in the internal side is due to a favorable on average current passage, forming thicker oxide. Anodized Ti takes different interference colors [43], depending on the thickness of growing oxide thin film thus on ΔV and other conditions [52], among which is blue. No dye red, or red interference color, was observed. As for the Al anode, the adsorption of dye anions must be very slow and their electro-adsorption ineffective.

In the Ti anode the oxygen release is much faster than in Al. Any kind of dye anion adsorption is physically hindered more by the oxygen released as nano-bubbles which then merge and expand into micro- and macro-bubbles [36]. The concentrations of released O^-, $O^{\bullet}$, $OH^{\bullet}$ and O_3 and their by-products in the attached layer and solution become higher. When dye anions or their fragments approach this layer, the chromophore groups and they as a whole decay faster. Thus, the access and adsorption of bulky anions/fragments is also more hindered and reactively prevented.

Cathodic Ti electrode: It was colored partly magenta, gently in both sides. The bulky dye anion with charge -6 cannot be electrochemically adsorbed on the (-) charged cathode. Only cationic fragments could do so. In the reductive cathode, the natural TiO_2 could be partly reduced, by the reactions noted previously, to various oxides with different colors, e.g. golden yellow (TiO), black (Ti_3O_4), dark violet (Ti_2O_3), blue (Ti_3O_5), etc. [48]. TiO_2 has low electronic conductivity (κ) at Ts around the ambient one, a little above 10^{-11} ohm^{-1} m^{-1}, but is a semiconductor and its conductivity rises with T. Ti_6O, Ti_5O, Ti_3O, Ti_2O and TiO have higher κs of the order of 10^{-1} ohm^{-1} m^{-1} [48].

The semiconductivity of TiO_2 on Ti metal favors the electronic over ionic current and, together with the higher κ of these oxides, it could favor the reduction of TiO_2, so that the initial TiO_2 layer thins and/or is altered to other oxide(s) but the oxide does not vanish. The oxide in the anode must be TiO_2, and in the cathode TiO_2 and/or other possible oxide(s) which is finally clarified in section 4. The magenta color in the cathode is interference color at other oxide thickness or the color of other type of oxide. The origin of the above colors is further studied below without using dye.

Ti anode – Ti cathode (reversed). The origin of colors in the Ti electrodes

The electrodes were carefully washed and their polarity was reversed. The wholly blue surface of anode and the more colored magenta surface of cathode before were placed opposite each other to ease the passage of current through them. To avoid T rise, 500 ml solution, with c_d = 0 and c_s = 0.1 M, was electrolyzed, using PS_1 galvanostatically up to 10.76 min and then potentiostatically up to 40 min. For t = 0–10.76 min, I = 0.5 A and ΔV = 14–35.2 V and for t =10.76–20.5–37–40 min, I = 500–250–60–57 mA and ΔV ≈ 35.2 V. Due mainly to the much lower $I\Delta V$ than in section 2 and higher volume of solution and heat transfer surface, T ≈ 25 °C at t = 0–40 min. Hereafter, for ease P_{an} and P_{ca} were found using the reference electrode. At t = 40 min, P_{an} = 33.615 V, $-P_{ca}$ = 1.464 V and $\Delta V_{bs} = \Delta V - P_{an} + P_{ca}$ = 0.121 V.

From κ_s, Table 1, ΔV_{bs} is found ≈ 0.396 V. The difference is tolerable for such low ΔV_{bs} and $\Delta V_{bs}/\Delta V$ values, validating the two methods of the approximate determination of ΔV_{bs}. The rise of ΔV at t = 0–10.76 min and fall of I at t = 10.76–40 min, while at the end I is low and P_{an} is high, show that TiO_2 thickened in the anode. The release of O_2 and H_2 in the electrodes was intensive up to t = 10.76 min, so H_2O decay is the main process, after which it declined with t.

$-P_{ca}$ exceeds much the H_2 overpotential on the Ti cathode ≈ 0.544 V [27]. So, a thin oxide layer still exists on the cathode and/or the nature of remaining oxide changed to more conductive form(s). Additional color observations:

How to cite this article: Patermarakis G. Discoloration of C.I. Reactive Red 120 Solutions by Electrochemical Treatment Using Anodic Electrodes of Al and Ti with and Pt without Surface Oxide Layer. Curr Trends Fashion Technol Textile Eng. 2023; 8(3): 555740. DOI: 10.19080/CTFTTE.2023.08.555740

Anodic Ti electrode (before magenta cathode): The internal and external surfaces became blue, locally very intensive, verifying the formation of thicker oxide film that displays blue interference color. The final thickness of oxide in the cathode in section 2, that equals the initial here, must be lower than the initial native passive layer thickness (section 2). In view of the final color of cathode in section 2 and the smaller oxide thickness in it, the thinner initial thickness here favors a more uniform oxide growth in both surfaces. The present conditions favored the growth of thicker on average oxide in the anode than in section 2. Lower T and sulphate concentration slowed Ti^{4+} solvation.

Cathodic Ti electrode (before blue anode): The internal surface remained blue, so the reduction of initial TiO_2 was not complete up to 40 min. Presumably the thicker oxide initially impeded to some extent the passage of current. The other side was colored locally magenta. This color cannot be due to dye anion or its rather impossible cationic fragment(s). It could come from reduction of the preexisting TiO_2 film to a thinner with this interference color and/or to other oxide(s) with this color. Blue is interference color. Magenta is such or the color of other Ti oxide(s), finally clarified below.

Ti anode – Ti cathode (reversed). Discoloration of dye solution

520 ml of solution with c_d = 48.08 mg dm^{-3} and c_s = 0.0385 M was electrolyzed using PS_2 at I = 0.5 A up to t = 3 hours where the discoloration was completed while ΔV was 71–139 V and $T \approx 25$ °C. At these low T and c_s, ΔV up to t = 10.76 min is much higher than in the section 3. This is due mainly to the higher P_{an} related to a higher mean thickness of TiO_2 grown in the anode, and secondarily to the higher ΔV_{bs} that is estimated ≈ 8.286 V, while the rise of $P_{an} + \Delta V_{bs}$ much exceeds the fall of $-P_{ca}$ due to the thinning of oxide and/or to a possible change of its nature in the cathode. In the anode the oxide thickens with increasing t and decreasing T and c_s. The decrease of T and c_s slows down the ejection and solvation of Ti^{4+} and $I_{a,c}$ falls, while $I - I_{a,c} = I_{a,a} + I_{a,e}$, responsible for oxide growth and oxygen release, rises.

The initial pH was 7.02. Due to the contained Na_2SO_4, ΔpH = 0.253 [26]. The calculated pH = 6.75 + 0.253 = 7.00 ≈ 7.02. After electrolysis, pH = 7.1. When $n_1 << n_2$ the total consumption of H^+ by reaction (9) is small, (6) occurs almost exclusively and the pH changes little. The final colors of the anode and cathode are shown in Figure 5.

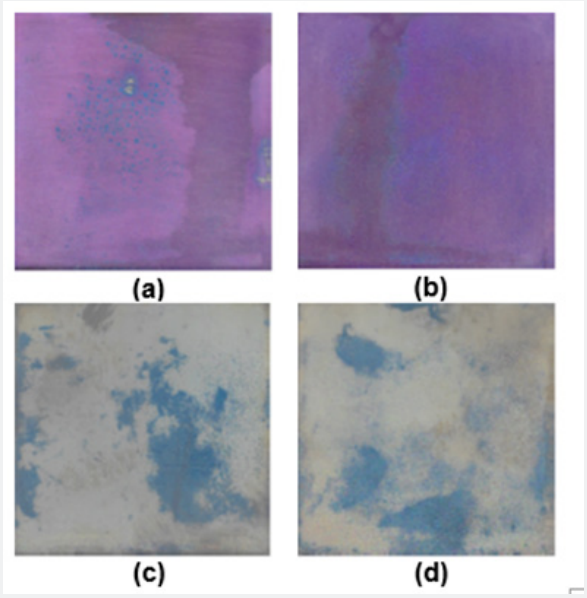

Figure 5: The two surfaces 5×5 cm2 of anode, (a) and (b), and of cathode, (c) and (d), and their colors after electrolysis in dye solution containing Na2SO4.

f5

Anodic electrode (before blue + magenta cathode): Now all its surface became intensively magenta with small, spots-like, blue regions, Figure 5a–b. Also, many other intermediate hues appeared. If the initial locally magenta color was due to oxide(s) with oxidation number < 4, in the strongly oxidative anode and for the long t employed this (they) should become TiO_2. So, the magenta color in the anode or cathode after electrolysis, sections 2–4, is an interference color exhibited by the thin oxide film. The blue and magenta colors appear, or reappear, at different oxide thicknesses.

Cathodic electrode (before blue anode): It remained blue

How to cite this article: Patermarakis G. Discoloration of C.I. Reactive Red 120 Solutions by Electrochemical Treatment Using Anodic Electrodes of Al and Ti with and Pt without Surface Oxide Layer. Curr Trends Fashion Technol Textile Eng. 2023; 8(3): 555740. DOI: 10.19080/CTFTTE.2023.08.555740

at the before intensively blue areas and almost discolored in the larger surface area where it was slightly blue, Figure 5c–d. In the reductive cathode, a partial reduction and thinning of TiO_2 occurred to thicknesses different than that showing magenta interference color. The above explanations were further confirmed by ohm-metric tests. The surface of cathode showed high conductivity, approaching that of Ti metal, while that of anode was very poorly conductive. The results in sections 2–4 verify the expected dependence of oxide thicknesses and interference colors in the anode and cathode on the initial ones and on t, T and c_s of electrolysis.

Figure 4a-d show inhomogeneous surfaces. Smooth area always coexists with topo-electrochemical corrosion (pitting) sites appearing when Ti is anode. In the cathode here, Figure 5c-d, some regions in both areas show blue color while the pitting corrosion sites are generally blue up to dark blue or black or colorless. This corrosion first appeared during electrolysis in section 3. In smooth areas, mostly oxygen release and much less Ti oxidation to TiO_2 took place. In the much smaller pitting corrosion area, the faster Ti oxidation gave mainly Ti^{4+} ejected in the solution and secondarily oxide. The local intensive burning/electropolishing for Al anode corresponds to the pitting corrosion in small areas for Ti one. The surface inhomogeneity is related to a distribution of local j. When Ti is cathode (this section) and H_2 release is the main process, the oxide thins everywhere in both areas and the surface details become clearer.

The anode surface, Figure 5a-b, shows larger mean surface density of pitting corrosion sites as it has become anode for longer time and higher mean T (sections 2 and 4). Mainly in the pitting corrosion and secondly in the smooth area, the surface appearance is more complex than in the cathode, due to higher density of pitting corrosion sites and many hues of blue or other color in these sites and of magenta in the remaining area. The metallurgical defects expand the inhomogeneity on each face of the electrodes.

The results (sections 1–4) suggest: (i_1) Absence of physical-, chemical- or electro-adsorption of dye in the electrodes, due to: ($i_{1,1}$) The large size of dye anions so that the simultaneous adsorption of suitable atoms, groups etc. is impossible or slow. Indeed, the PAAF adsorbent takes up dye very slowly [4] and this must hold for TiO_2 too. ($i_{1,2}$) Gases released in the electrodes hinder the approach of bulky anions. ($i_{1,3}$) If they approach the attached layer, the active species that accumulate in it, mainly on the anode, destroy the chromophore groups. A minor such effect of $H^{\bullet}$ and other species/radicals formed near the cathode is not excluded. (ii_1) The dye does not decay on the surface of electrodes or does so negligibly. (iii_1) Discoloration occurs almost exclusively in the solution. (iv_1) The rise of T accelerates it. (v_1) The active species are associated with the oxides on the Al and Ti anodes. This is tested further using Pt(Ti) electrodes.

Anode Pt(Ti) – cathode Pt(Ti). Discoloration of dye solution

520 ml solution with c_d = 48.08 mg dm^{-3} and c_s = 0.0385 M was electrolyzed using PS_1 at I = 0.5 A for t = 3 hours. ΔV was 9.8–10.1 V and $T \approx 25$ °C. For ΔV = 9.8 V, P_{an} = 1.85 V and $-P_{ca}$ = 0.81 V and for ΔV = 10.1 V, P_{an} = 1.925 V and $-P_{ca}$ = 1.065 V. Then, $\Delta V_{bs} = \Delta V - P_{an} + P_{ca}$ = 7.14 and 7.11 V. P_{an} is low because a clear growth of oxide film on Pt surface does not occur and only oxygen release does [27]. Initially pH = 7.02 (as in section 4) and finally 6.02. This is the first time the pH has decreased. The discoloration of solution was trivial, ≈ 4%. In Pt cathode the rate of H_2 release is faradaic, reaction (2). At pH ≈ 7 the release of O_2 in the Pt anode occurs in two ways [27], reactions (6) and

$$2OH^- \rightarrow (1/2)O_2 + H_2O + 2e^-, \quad (11)$$

with faradaic total rate. Reactions (2), (3) and the overall reaction at the anode and cathode $H_2O \rightarrow H_2 + (1/2)O_2$ show that the pH must remain constant irrespective of reaction(s) taking place in the anode, (6), or (11), or both as here. Its fall implies that a small fraction of dye anions decays to acidic species. The trivial discoloration efficacy shows that the active species in Pt(Ti) – Pt(Ti) differ from those in Al – Pb and Ti – Ti systems as to their kind and/or concentrations and thus kind and intensity of action. With the Pt anode, an oxidative decay of a small fraction of dye anions into rather large fragments must occur, but with the Al and Ti anodes extensive and deeper destruction occurs. Other observations:

Anodic electrode: Its color did not show any difference from the initial.

Cathodic electrode: Its side opposite the anode became darker with magenta somewhat color mainly at the edges and in the form of thin linear upwards regions with tiny area. Local intense release of H_2, and drop in pH, may favor a small degree of dimerization/aggregation and/or flocculation/coagulation of dye that is deposited [4] but with altered color.

Anode Pt(Ti) – cathode Pt(Ti) (reversed). Discoloration of dye solution

To increase the concentration of dye-destructive species, a lower volume of solution 150 ml with c_d = 41.67 mg dm^{-3} and c_s = 0.167 M was electrolyzed at I = 0.5 A (using PS_1) while it was $T \approx 25$ °C and ΔV = 5–6 V. By t = 60 min, discoloration was only ≈ 9%, predicting ≈ 27% (at most) at t = 3 hours. This again confirms the different nature and/or lower concentration and activity of the active species in the Pt(Ti) – Pt(Ti). Other observations:

Anodic Pt(Ti) electrode: Discoloration of the anode due to discoloration/decay of preexisting deposited dye.

Cathodic Pt(Ti) electrode: As in section 5, it became partly magenta in a negligible portion of surface.

How to cite this article: Patermarakis G. Discoloration of C.I. Reactive Red 120 Solutions by Electrochemical Treatment Using Anodic Electrodes of Al and Ti with and Pt without Surface Oxide Layer. Curr Trends Fashion Technol Textile Eng. 2023; 8(3): 555740. DOI: 10.19080/CTFTTE.2023.08.555740

As no oxide is formed in the Pt anode and only adsorbed oxygen-based species can exist [27], the oxygen release is faster even to a small extent than in the Ti anode where oxygen release, oxide formation and Ti^{4+} ejection coexist. Also, as noted in section 1.1 the release of oxygen in the Al anode is hardly visible. The oxygen release in the Pt anode is thus faster, but much less effective to the discoloration of dye solution, than in the Al and Ti anodes. The mechanism of oxygen release in the Al and Ti anodes [36] predicts that O_2 together with the species O^-, $O^{\bullet}$, $OH^{\bullet}$ (short-lived and short-range acting) and O_3 (long-lived and long-range acting) are formed and enter the solution. If such species are indeed formed in Pt anode, their formation rate must be tiny compared to that in the Al and Ti anodes.

In the latter anodes, O_2, O^-, $O^{\bullet}$, $OH^{\bullet}$ and O_3 are formed by certain 3D processes in the oxide bulk [36]. In the Pt anode the formation of O_2 is mostly a 2D surface process. Also, the 3D formation of O_3 seems to be more effective than 2D if any. The very different efficiencies to dye solution discoloration come mainly from those dissimilar mechanisms. If $H^{\bullet}$ were the main active species, the efficiencies around the Pt, Pb and Ti cathodes would be comparable. If the main active species were those coming from dissolved O_2 in the vicinity of cathodes, this would hold at least for Pt and Ti cathodes too. These are not the cases. Thus, the active species come indeed mostly from the anodes.

Comparison of the efficiencies of anode – cathode systems in terms of consumed electric charge and energy

The results show that the discoloration of dye solution is a chemical process occurring in its bulk, rather than an electrochemical in the interfaces. The comparison of the employed systems, as regards the discoloration efficiency (*d.e.*), the mean rate of discoloration and the *Q* and energy (*E*) required, appears in Table 2. *E* is calculated from the estimated mean ΔV, E = (mean ΔV) Q. For *d.e.* = 1, the mean rate is higher for the Ti –Ti systems where it also increases with the mean *T*, followed by the Al – Pb system. The higher rate for the Ti – Ti systems is obviously related to the higher rate of evolution of oxygen and related species in the anode. The Pt(Ti) – Pt(Ti) systems show very low *d.e.* values. For *d.e.* = 1, $Q[m_d(d.e.)]^{-1}$ is lower in the Ti – Ti systems for which it decreases appreciably with the mean *T*. $E[m_d(d.e.)]^{-1}$ is much lower in the Al – Pb system, while in the Ti – Ti systems it is affected by both c_s and *T*. Their values are much larger in the Pt(Ti) – Pt(Ti) systems, so they are generally practically ineffective.

Table 2: Concentration of dye, c_d, initial mass of dye, m_d, concentration of Na_2SO_4, c_s, electrochemical treatment time, *t*, temperature, *T*, voltage, ΔV, mean ΔV during electrochemical treatment, discoloration efficiency, *d.e.*, mean discoloration rate, $m_d(d.e.)t^{-1}$, electric charge, *Q*, and energy, *E*, consumed during electrochemical treatment, $Q[m_d(e.d.)]^{-1}$ and $E[m_d(e.d.)]^{-1}$, for the applied electrochemical systems Al – Pb, Ti – Ti and Pt(Ti) – Pt(Ti).

Anode-cathode system	c_d/mg dm^{-3}	m_d/mg	c_s/mol dm^{-3}	t/min	T/°C	ΔV/V	Mean ΔV/V
1. Al – Pb	47.5	9.5	0.05	0–60–120	25–57–57	34.0–24.3–24.3	26.725
2. Ti – Ti	50	10	0 ($t \le 30$ min), ≈ 1 ($t > 30$ min)	0–30–60	25–62–62	150–160–170	160
3. Ti – Ti	48.08	25	0.0385	0–90–180	25	71–105–139	106
4. Pt(Ti) – Pt(Ti)	48.08	25	0.0385	0–90–180	25	9.8 –9.95–10.1	9.95
5. Pt(Ti) – Pt(Ti)	41.67	6.25	0.167	0–60	25	5.0–6.0	5.5
Anode-cathode system	***I*/A**	***d.e.***	$m_d(d.e.)t^{-1}$/ mg min^{-1}	***Q*/C**	$Qm_d^{-1}(e.d.)^{-1}$/ C mg^{-1}	***E*(mean ΔV) *Q*/J**	$Em_d^{-1}(e.d.)^{-1}$ / J mg^{-1}
1. Al – Pb	0.5	1	0.079	3600	379	96210	10127.4
2. Ti – Ti	0.5	1	0.167	1800	180	288000	28800
3. Ti – Ti	0.5	1	0.139	5400	216	572400	22896
4. Pt(Ti) – Pt(Ti)	0.5	0.04	0.0056	5400	5400	53730	1343250
5. Pt(Ti) – Pt(Ti)	0.5	0.09	0.0094	1800	3200	9900	195555.6

How to cite this article: Patermarakis G. Discoloration of C.I. Reactive Red 120 Solutions by Electrochemical Treatment Using Anodic Electrodes of Al and Ti with and Pt without Surface Oxide Layer. Curr Trends Fashion Technol Textile Eng. 2023; 8(3): 555740. DOI: 10.19080/CTFTTE.2023.08.555740

The different *d.e.*s of Al, Ti and Pt anodes come from: (i_2) The different mechanisms of evolution of active species and their nature in Al and Ti and in Pt. (ii_2) Different rates of evolution of that species in Al, Ti and Pt and species concentrations in the solution. The full elucidation of (iii) needs further specific analytical work.

Conclusion

1. The anodic electrodes on which oxide is developed, such as Al and Ti, are effective in the discoloration of RR 120 dye solutions. Their effectivity is attributed to a similar mechanism of electronic current release. It involves the polarization and destabilization of oxide lattice O^{2-} ions, concurrent solvation of metal cations, continuous renewal of a thin oxide layer between the metal and electrolyte [36], and the formation O^-, $O^\bullet$, $OH^\bullet$, O_2 and O_3 species that enter the attached layer and solution and are the main initial species responsible for the discoloration and destruction of the dye.

2. These occur almost solely in the bath solution and not on the electrode surfaces and are enhanced with increasing temperature. At comparable electrolysis conditions, their rates are higher for Ti anode. But, the use of Al is much more effective as regards ΔV and energy requirements. The Ti anode and cathode show interference colors wholly or partly on the surface, blue or magenta at various tones, due to thin oxide layers. The consumption of Al and the mean thickness of oxide in its entire surface are much higher than those for Ti, while the Ti anode shows pitting corrosion.

3. The electrochemical treatment of dye solution with a Pt anode, where only oxygen is adsorbed and oxide does not grow, is negligibly effective. This is due to the different mechanism of release of oxygen and related active species. In the Pt anode their release is a surface process and not a bulk one as in the oxide layers on Al and Ti that favors more the formation of the O^-, $O^\bullet$, $OH^\bullet$ and O_3 active species. The role of cathodes and related processes is marginal.

The optimization of the process using Al and Ti anodes, and possibly other materials that form oxide layers during anodizing, may result in a much faster discoloration and total mineralization of solutions of RR 120 and other azo-reactive dyes. Novel methods for a radical solution of textile effluent treatment problem are expected to be revealed.

References

1. Georgiou D, Kalis M, Patermarakis G, Vassiliadis AA (2017) Destruction of Azo-Reactive Dyes by Ozonation and the Synergetic Effect of a Radiofrequency Alternating Electric Field Inductance Device. Current Trends Fashion Technology and Textile Engineering 1(2): 42-47.
2. Santos DCD, Adebayo MA, Pereira SFP, Prola LDT, Cataluña R, et al. (2014) New carbon composite adsorbents for the removal of textile dyes from aqueous solutions: Kinetic, equilibrium, and thermodynamic studies. Korean J Chem Eng 31(8): 1470-1479.
3. Çelekli A, Al-Nusimi AI, Bozkurt H (2019) Adsorption Kinetic and Isotherms of Reactive Red 120 on Moringa oleifera seed as an eco-friendly process. Journal of Molecular Structure 1195: 168-178.
4. Patermarakis G, Vassiliadis AA (2023) Mechanism of C.I. Reactive Red 120 Uptake from Solution by Anodic Alumina Films. Curr Trends Fashion Technol Textile Eng 8(3): 555737.
5. Harrelkas F, Azizi A, Yaacoubi A, Benhammou A, Pons MN (2009) Treatment of textile dye effluents using coagulation flocculation coupled with membrane processes or adsorption on powdered activated carbon. Desalination 235(1-3): 330-339.
6. Georgiou D, Aivasidis A (2012) Cotton-textile wastewater management: investigating different treatment methods. Water Environ Res 84(1): 54-64.
7. Sarayu K, Sandhya S (2012) Current Technologies for Biological Treatment of Textile Wastewater-A Review. Appl Biochem Biotechnol 167(3): 645-661.
8. Gupta VK, Khamparia S, Tyagi I, Jaspal D, Malviya A (2015) Decolorization of mixture of dyes: A critical review. Glob J Environ Sci Manage 1(1): 71-94.
9. Roulia M, Vassiliadis AA (2009) Clay-catalyzed phenomena of cationic-dye aggregation and hydroxo-chromium oligomerization. Microporous and Mesoporous Materials 122(1-3): 13-19.
10. Roulia M, Vassiliadis AA (2008) Sorption characterization of a cationic dye retained by clays and perlite. Microporous and Mesoporous Materials 116(1-3): 732-740.
11. Georgiou D, Melidis P, Aivasidis A, Gimouhopoulos K (2002) Degradation of azo reactive dyes by UV radiation in the presence of hydrogen peroxide. Dyes Pigments 52(2): 69-78.
12. Soares PA, Silva TFCV, Manenti DR, Souza SMAGU, Boaventura RAR, et al. (2014) Insights into real cotton-textile dyeing wastewater treatment using solar advanced oxidation processes. Environmental Science and Pollution Research Int 21(2): 932-945.
13. Asghar A, Raman AAA, Daud WMAW (2015) Advanced oxidation processes for in-situ production of hydrogen peroxide/hydroxyl radical for textile wastewater treatment: a review. J Cleaner Production 87: 826-838.
14. Cardoso JC, Bessegato GG, Zanoni MVB (2016) Efficiency comparison of ozonation, photolysis, photocatalysis and photoelectrocatalysis methods in real textile wastewater decolorization. Water Res 98: 39-46.
15. Cui M, Jang M, Cho SH, Elena D, Khim J (2011) Enhancement in mineralization of a number of natural refractory organic compounds by the combined process of sonolysis and ozonolysis (US/O_3). Ultrasonic Sonochemistry 18(3): 773-780.
16. Sathishkumar P, Mangalaraja RV, Anandan S (2016) Review on the recent improvements in sonochemical and combined sonochemical oxidation processes - A powerful tool for destruction of environmental contaminants. Renewable and Sustainable Energy Reviews 55: 426-454.
17. Babu SG, Ashokkumar M, Neppolian B (2016) The Role of Ultrasound on Advanced Oxidation Processes. Top Curr Chem (Cham) 374(5): 75.
18. Sugiarto AT, Ito S, Ohshima T, Sato M, Skalny JD (2003) Oxidative decoloration of dyes by pulsed discharge plasma in water. Journal of Electrostatics 58(1-2): 135-145.
19. Zhang L, Sun B, Zhu X (2009) Organic dye removal from aqueous solution by pulsed discharge on the pinhole. Journal of Electrostatics 67(1): 62-66.

How to cite this article: Patermarakis G. Discoloration of C.I. Reactive Red 120 Solutions by Electrochemical Treatment Using Anodic Electrodes of Al and Ti with and Pt without Surface Oxide Layer. Curr Trends Fashion Technol Textile Eng. 2023; 8(3): 555740. DOI: 10.19080/CTFTTE.2023.08.555740

20. Jiang B, Zheng J, Qiu S, Wu M, Zhang Q, et al. (2014) Review on electrical discharge plasma technology for wastewater remediation. Chemical Engineering Journal 236: 348-368.

21. Koutahzadeha N, Esfahania MR, Arcea PE (2016) Removal of Acid Black 1 from water by the pulsed corona discharge advanced oxidation method. Journal of Water Process Engineering 10: 1-8.

22. Shah AR, Tahir H (2019) Optimization of Sono-Electrocoagulation Process for the Removal of Dye Using Central Composite Design. Mehran University Research Journal of Engineering & Technology 38(2): 399-414.

23. Patermarakis G, Fountoukidis E (1990) Disinfection of water by electrochemical treatment. Water Research 24(12): 1491-1496.

24. Neta P (1972) Reactions of hydrogen atoms in aqueous solutions. Chem Rev 72(5): 533-543.

25. Colour Index, The Society of Dyers and Colourists and American Association of Textile Chemists and Colorists.

26. Dobos D (1975) Electrochemical Data: A Handbook for Electrochemists in Industry and Universities. Elsevier.

27. Antropov LI (1972) Theoretical Electrochemistry, Mir Publishers, Moscow.

28. Sheasby PG, Pinner R (2001) The Surface Treatment and Finishing of Aluminium and Its Alloys, sixth ed. ASM International & Finishing Publications Ltd, USA-UK.

29. Lee W, Park SJ (2014) Porous anodic aluminum oxide: anodization and templated synthesis of functional nanostructures. Chem Rev 114(15): 7487-7556.

30. Keller F, Hunter MS, Robinson DL (1953) Structural Features of Oxide Coatings on Aluminum. Journal of The Electrochemical Society 100(9): 411-419.

31. Young L (1961) Anodic Oxide Films, Academic Press, London.

32. Diggle JW, Downie TC, Goulding CW (1969) Anodic oxide films on aluminum. Chemical Reviews 69(3): 365-405.

33. Patermarakis G, Moussoutzanis K (2011) Transformation of porous structure of anodic alumina films formed during galvanostatic anodising of aluminium. Journal of Electroanalytical Chemistry 659(2): 176-190.

34. Patermarakis G (2020) The multimodal dependence of anodic alumina film porous nanostructure on anodizing potential. Curr Top Electrochem 22: 1-17.

35. Patermarakis G (2014) Thorough electrochemical kinetic and energy balance models clarifying the mechanisms of normal and abnormal growth of porous anodic alumina films. Journal of Electroanalytical Chemistry 730: 69-85.

36. Patermarakis G (2021) A novel theory on the mechanisms of generation, transport and release of oxygen gas and electronic current in anodic alumina film during Al anodizing. Curr Top Electrochem 23: 97-115.

37. Atkins P (2010) Physical Chemistry, Oxford University Press.

38. Weast RC (Ed) (1980) Handbook of Chemistry and Physics, (60th Edn), CRC Press, Boca Raton.

39. Patermarakis G, Plytas J (2016) A novel theory interpreting the extremes of current during potentiostatic anodizing of Al and the mechanisms of normal and abnormal growth of porous anodic alumina films. Journal of Electroanalytical Chemistry 769: 97-117.

40. Patermarakis G, Moussoutzanis K (2009) Development and application of a holistic model for the steady state growth of porous anodic alumina films. Electrochimica Acta 54(9): 2434-2443.

41. Vogel AI (1976) Macro and Semimicro Quantitative Analysis, Longman, London.

42. Alexeyev VN (1980) Qualitative Chemical Analysis, Mir Publishers, Moscow.

43. Young L (1961) Anodic Oxide Films, Academic Press, London.

44. Qing G, Abolhassani M, Daneshpour R, Foster SL, Matlock M, et al. (2021) Disinfection of Irrigation Water Using Titanium Electrodes. Journal of The Electrochemical Society 168(6): 063502.

45. Lausmaa J, Kasemo B, Mattsson H (1990) Surface spectroscopic characterization of titanium implant materials. Applied Surface Science 44(2): 133-146.

46. Prando D, Brenna A, Diamanti MV, Beretta S, Bolzoni F, et al. (2017) Corrosion of Titanium: Part 1: Aggressive Environments and Main Forms of Degradation. J Appl Biomater Funct Mater 15(4): e291-e302.

47. Emsley J (2011). "Titanium". Nature's Building Blocks: An A-Z Guide to the Elements. Oxford University Press Inc., New York, USA.

48. Samsonov GV (1973) The Oxide Handbook, IFI/Plenum, New York.

49. Davies CW (1967) Electrochemistry, Newness, London.

50. Alexeyev VN (1985) Quantitative Analysis, Mir Publishers, Moscow.

51. Unpublished data.

52. Alwitt RS (2002) Electrochemistry Encyclopedia. Chemical Engineering Department, Case Western Reserve University, U.S.

How to cite this article: Patermarakis G. Discoloration of C.I. Reactive Red 120 Solutions by Electrochemical Treatment Using Anodic Electrodes of Al and Ti with and Pt without Surface Oxide Layer. Curr Trends Fashion Technol Textile Eng. 2023; 8(3): 555740. DOI: 10.19080/CTFTTE.2023.08.555740

DOI: 10.19080/CTFTTE.2023.08.555740

How to cite this article: Patermarakis G. Discoloration of C.I. Reactive Red 120 Solutions by Electrochemical Treatment Using Anodic Electrodes of Al and Ti with and Pt without Surface Oxide Layer. Curr Trends Fashion Technol Textile Eng. 2023; 8(3): 555740. DOI: 10.19080/CTFTTE.2023.08.555740